

sium, decarbomethoxylation, reduction, aromatization, decarboxylation, and devinylation to give rise to a group of free base porphyrins of the DPEP homologous series ($308 + 14m$, where m is 2 or greater). Porphyrins of the DPEP series retain the isocyclic ring characteristic of chlorophyll [E. W. Baker, in *Organic Geochemistry*, G. Eglinton and M. T. J. Murphy, Eds. (Springer Verlag, Berlin, 1969), p. 480]. The short series of DPEP-type free base porphyrins, usually consisting of C_{32} to C_{29} , then becomes chelated with either nickel or vanadyl, resulting in compounds stable in a field of increasing thermal stress. Subsequent reactions fall into the realm of early catagenesis. With increasing temperature ($\sim 50^\circ\text{C}$) the metalloporphyrins of the DPEP series are gradually converted to members of the etio series ($310 + 14n$, where $n = 1$ or greater) by rupture of the isocyclic ring followed by dealkylation (loss of methylene groups from the tetrapyrrole ring) and in special cases transalkylation. "Transalkylation" refers to the proposed free radical mechanism by which methylene units can be added (alkylation) or removed (dealkylation) from the tetrapyrrole ring. This process results in metalloporphyrins having homologous series in the range C_{33} to C_{27} . Since the reactions proceed with increasing temperature, chlorophyll diagenesis serves as a paleothermometer.

- Core samples were stored frozen until the time of analysis; mixtures of acetone and methanol (9:1) were used for ball mill extraction of pigments. Metalloporphyrins were then isolated from the crude extractions by chromatography over neutral alumina (grade III). Nickel and cop-

per porphyrins cochromatograph with a mixture of cyclohexane and benzene (1:1), whereas the more polar vanadyl porphyrins can be eluted with a mixture of benzene and tetrahydrofuran (1:1). Repeated chromatography of the porphyrins yields relatively pure fractions for electronic and solid probe mass spectrometry.

- E. W. Baker, M. S. Brookhart, A. H. Corwin, *J. Am. Chem. Soc.* **86**, 4587 (1964); J. C. W. Chien, *ibid.* **100**, 1310 (1978).
- E. W. Baker, S. E. Palmer, W. Y. Huang, *Initial Rep. Deep Sea Drill. Proj.* **40**, in press; *ibid.* **41**, 825 (1977); S. E. Palmer and E. W. Baker, *ibid.* **50**, in press.
- Shipboard party, Leg 40, *Geotimes* **20** (No. 6), 22 (1975); shipboard party, Leg 41, *ibid.* **20** (No. 7), 18 (1975); shipboard party, Leg 50, *ibid.* **22** (No. 4), 24 (1977).
- The Black Sea, presently an isolated inland sea with anoxic bottom waters, contains a complex sequence of Pleistocene sediments which reflect the climatic influence imposed by alternating glacial and interglacial stages. Anoxic conditions have existed in the Black Sea for approximately the last 7300 years. Before this, the basin underwent evaporitic, brackish water, and lacustrine phases [3]; D. A. Ross, in *The Geology of Continental Margins*, C. A. Burk and C. L. Drake, Eds. (Springer-Verlag, New York, 1974), p. 669].
- This research was supported by the Oceanography Section of the National Science Foundation under grants OCE 74-12438 A02 and OCE 77-072773. We thank G. DeMott for laboratory assistance.

18 January 1978; revised 28 March 1978

Noble Gases in the Murchison Meteorite:

Possible Relics of s-Process Nucleosynthesis

Abstract. *The Murchison carbonaceous chondrite contains a new type of xenon component, enriched by up to 50 percent in five of the nine stable xenon isotopes, mass numbers 128 to 132. This component, comprising 5×10^{-5} of the total xenon in the meteorite, is released at 1200° to 1600°C from a severely etched mineral fraction, and probably resides in some refractory mineral. Krypton shows a similar but smaller enrichment in the isotopes 80 and 82. Neon and helium released in the same interval also are quite anomalous, being highly enriched in the isotopes 22 and 3. These patterns are strongly suggestive of three nuclear processes believed to take place in red giants: the s process (neutron capture on a slow time scale), helium burning, and hydrogen shell burning. If this interpretation is correct, then primitive meteorites contain yet another kind of alien, presolar material: dust grains ejected from red giants.*

Noble gases in carbonaceous chondrites show complex isotopic patterns, dating back to the beginning of the solar system or even beyond. To resolve these patterns into their components, two techniques have proved especially useful: extraction of gases by stepwise heating, and mineral separation by chemical techniques. We have combined both in the present study.

One of the more enduring puzzles in this field is a xenon component enriched in both heavy and light isotopes (1-4), which has been attributed to fission of a superheavy element (5), or to nuclear processes in a supernova (2, 3). It is commonly designated by the acronym CCFXe (for carbonaceous chondrite fission xenon), although its fission origin has not yet been proved. This component resides mainly in chromite and amorphous carbon (4, 6, 7). These

phases can be isolated by dissolving the bulk of the meteorite in HCl-HF, and etching the residue (0.5 to 2 percent) with oxidizing reagents to remove two other phases that contain large amounts of ordinary trapped (or "primordial") xenon: the organic polymer and "phase Q," a poorly characterized mineral that may be an Fe,Cr-sulfide (5, 8).

In our previous study of the Murchison C2 chondrite (7), we were only partly successful in removing trapped xenon, judging from the modest enrichment in the heavy xenon isotopes. The highest $^{136}\text{Xe}/^{132}\text{Xe}$ ratio was only 0.441, higher than the ratio in trapped Xe (0.310) but lower than the highest value found for the Allende meteorite [0.626 (6)]. We therefore devised a new procedure for removal of polymer and Q, involving alkaline oxidants such as $\text{NaOH} + \text{H}_2\text{O}_2$ or NaClO (9), in addition to the fuming

nitric acid used previously. This procedure indeed dissolved ~ 90 percent rather than 55 percent of the residue, and left a sample (designated 1C10) that yielded a $^{136}\text{Xe}/^{132}\text{Xe}$ ratio as high as 0.53 on stepwise heating. But the fractions released at the highest temperatures showed some new and totally unexpected trends.

The large, 800°C xenon fraction (Table 1) seems to consist mainly of trapped xenon from the polymer, judging from the low release temperature and isotopic similarity to trapped meteoritic xenon (penultimate line in Table 1). The 1000° and 1100°C fractions show the usual traits of CCFXe: enrichments in the lightest three and heaviest two isotopes, and little change in the others, relative to ^{132}Xe . But starting with the 1200°C fraction, some new trends appear: isotopes 128 and 130 rise, whereas 129, 131, 134, and 136 fall, all to more extreme values than any observed in meteoritic or lunar samples in the 18 years since John Reynolds founded the field.

Although the two most anomalous fractions (1400° and 1600°C) are quite small, the anomaly is not an artifact of the blank correction. This correction is only 1 percent for the 1400°C fraction, and although it is larger (25 percent) for the 1600°C fraction, even the uncorrected ratios are quite anomalous (10).

It appears that a new kind of xenon component is present in the 1200° to 1600°C fractions. This can be verified by three-isotope plots, such as Fig. 1. On such a plot, mixtures of n components fall within an n -sided polygon of minimum area, whose vertices are the individual components. Xenon in carbonaceous chondrites normally behaves like a pseudobinary mixture, with all samples lying on a straight "mixing line" that joins trapped Xe (from Q and polymer) at the left and CCFXe (from chromite and carbon) off the scale to the right (11, 12). When air xenon is present, samples drift below the line, toward the atmospheric point.

All Murchison samples ever measured by us indeed lie on the mixing line, except for the 1100° to 1600°C fractions of Murchison 1C10. This deviation cannot be due to air xenon, because the points lie above rather than below the mixing line. Apparently these fractions contain a third xenon component, lying somewhere on the upper left in Fig. 1.

The isotopic pattern of this third component can be qualitatively inferred from the 1400° and 1600°C fractions (Table 1). Isotopes 128 and 130 are obviously enriched, and so is the normalizing isotope 132, judging from the parallel decrease of

the four isotopes 129, 131, 134, and 136. These four isotopes, as well as the two light isotopes 124 and 126, must be rare or absent in the new component; the amounts still present in these fractions probably come from the trapped component.

Of all plausible astrophysical processes, only the *s* process (neutron capture on a slow time scale) seems capable of producing such a pattern, enriched mainly in the *even*-numbered, *middle* isotopes. Fission or the *r* process (neutron capture on a rapid time scale) would produce only the unshielded isotopes 129 and 131 to 136. Spallation of heavier elements such as Ba or rare earths would make mainly the light, shielded isotopes 124, 126, and 128.

Accepting the idea that the new com-

ponent represents *s*-process xenon, we can try to derive its composition by assuming that it contains no $^{134,136}\text{Xe}$ at all. The amounts of trapped and fission xenon in each fraction are first calculated from the $^{134}\text{Xe}/^{136}\text{Xe}$ ratio, making use of the fact that this ratio differs greatly between these two components [trapped, 1.22 to 1.29; fission, 0.673 to 0.715 (7)], and are then subtracted from the gross spectrum. The resulting patterns for the new component are given in Table 2, for two extreme choices of the fission component (7). In Fig. 2, the average composition is compared with the range of theoretical estimates for the *s* process, from Clayton and Ward (13). The odd isotopes have large errors, but the even isotopes are rather consistent, and the mean, for both combinations of fission and trapped

components, falls within the range of the theoretical estimates.

Both the Murchison and the theoretical values show the same main features: absence of 124 and 126, predominance of even over odd isotopes, and increase in abundance with mass number. We have no good way of testing our assumption that isotopes 134 and 136 are absent in the new component. But it is reassuring that all three fractions give similar patterns after subtraction of quite different proportions of trapped and fission xenon.

Krypton shows similar but much smaller anomalies in the 1400° and 1600°C fractions. The effect is blurred by variations in the trapped and fission components, and is readily noticeable only for ^{82}Kr and perhaps ^{80}Kr in the 1600°C fraction (Table 3). But these two isotopes happen to be the very ones that are shielded by selenium isotopes and hence are made mainly by the *s* process (14). The amounts of anomalous ^{82}Kr , calculated by assumptions similar to those for Xe (15), are $0.2 \pm 0.1 \times 10^{-10}$ and $0.03 \pm 0.03 \times 10^{-10}$ cm³ STP/g for the 1400° and 1600°C fractions. The $^{80}\text{Kr}/^{82}\text{Kr}$ ratio in the 1600°C fraction is 0.2 ± 0.3 . The corresponding $^{82}\text{Kr}/^{130}\text{Xe}$ ratios are 0.3 and 0.2, much below the solar-system ratio of 24 (14).

The neon data (Table 4) show much larger anomalies, which are best visualized in a graph (Fig. 3). Meteoritic neon usually can be represented as a mixture of three components: solar or "Ne-B" ($^{20}\text{Ne}/^{22}\text{Ne} \approx 13$), planetary or "Ne-A" ($^{20}\text{Ne}/^{22}\text{Ne} \approx 8.2$), and cosmic-ray-pro-

Fig. 1. Xenon in mineral residues of the Murchison meteorite [(7) and this work]. Increasing harshness of chemical treatment is indicated by increasing polygonality of symbols; percentages indicate the fraction of the original weight remaining after treatment. Most samples fall on the mixing line between trapped and fission (CCF) xenon, but the 1100° to 1600°C fractions of 1C10 lie above the line, indicating the presence of a new component enriched in ^{130}Xe . The effect of the blank correction is shown for the 1600°C sample of 1C10; it is invisible on the scale of this graph for all others. (*) Atmospheric composition.

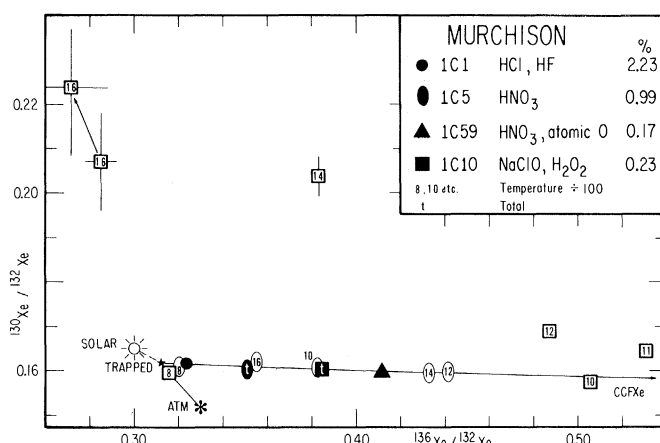


Table 1. Xenon in severely etched residue 1C10 of the Murchison meteorite (9, 41). The $^{136}\text{Xe}_f$ is possibly fission-derived ^{136}Xe . Corrections for hot blanks were negligible up to 1200°C, and were applied only to the 1400° and 1600°C fractions, where they comprised 1 and 25 percent of the observed ^{132}Xe signal (10).

Temperature (°C)	Concentration ($\times 10^{-10}$ cm ³ STP/g)*		^{124}Xe	^{126}Xe	^{128}Xe	^{129}Xe	^{130}Xe	^{131}Xe	^{134}Xe	^{136}Xe
	^{132}Xe	$^{136}\text{Xe}_f$								
800	861	6.7	0.4382 $\pm .0056$	0.3970 $\pm .0051$	8.095 $\pm .084$	105.31 $\pm .38$	15.94 $\pm .10$	82.16 $\pm .27$	37.97 $\pm .14$	31.55 $\pm .15$
1000	273	55	0.6560 $\pm .0013$	0.4788 $\pm .0099$	8.605 $\pm .098$	104.67 $\pm .37$	15.769 $\pm .074$	83.13 $\pm .39$	50.52 $\pm .25$	50.56 $\pm .31$
1100	144	33	0.661 $\pm .014$	0.513 $\pm .021$	8.88 $\pm .10$	104.59 $\pm .56$	16.47 $\pm .14$	83.01 $\pm .56$	52.17 $\pm .27$	53.06 $\pm .29$
1200	50	10	0.588 $\pm .012$	0.449 $\pm .016$	8.80 $\pm .15$	101.63 $\pm .56$	16.90 $\pm .19$	81.48 $\pm .34$	48.33 $\pm .34$	48.70 $\pm .42$
1400	10.9	1.3	0.493†	0.417†	10.07 $\pm .29$	94.2 ± 1.2	20.38 $\pm .45$	75.82 $\pm .93$	40.22 $\pm .36$	38.30 $\pm .28$
1600	1.6	0.08	0.559†	0.450†	10.97 $\pm .86$	77.7 ± 6.9	22.4 ± 1.6	62.5 ± 5.7	30.4 ± 1.8	27.2 ± 1.6
Total	1341	106	0.5126 $\pm .0039$	0.4283 $\pm .0045$	8.328 $\pm .059$	104.85 $\pm .26$	16.041 $\pm .068$	82.35 $\pm .20$	42.44 $\pm .11$	38.42 $\pm .12$
Solar			0.478	0.427	8.31	104.8	16.50	82.28	36.94	29.99
Trapped (7)			0.453	0.410	8.09	103	16.3	81.8	37.5	30.8
Air			0.357	0.335	7.14	98.3	15.17	78.77	38.82	33.00

*STP, standard temperature and pressure.

†Average of first two peak height measurements only.

duced or "cosmogenic" ($^{20}\text{Ne}/^{21}\text{Ne}/^{22}\text{Ne} \approx 0.85/0.92/1.00$), off scale to the right in Fig. 3. Several minor components have also been postulated, of which "Ne-E," characterized by very low but poorly known 20/22 and 21/22 ratios, is the most interesting, being located in what may be interstellar grains (16).

Most Murchison points fall within the A-B-cosmogenic triangle, although a few temperature fractions and an HNO_3 -soluble fraction (Q) are slightly displaced toward the Ne-E corner. But the 1200° and 1400°C fractions of 1C10 fall well below the triangle, and hence must contain a component rich in ^{22}Ne . The collinear trend of the 1000° to 1200°C fractions, which points toward the origin, suggests that this component could be a pure ^{22}Ne spike. However, the trend of the 1200° and 1400°C fractions alone implies a more conventional Ne-E component, with finite amounts of the other two isotopes but a 21/22 ratio below the present upper limit of 0.0211 (16). Experimentally, these two possibilities are hard to distinguish, because even small amounts of the ubiquitous trapped and cosmogenic neon components would add enough ^{20}Ne and ^{21}Ne to a pure ^{22}Ne spike to displace it from the origin. But whatever the nature of this anomalous neon component, it shows up in the same fractions where the anomalous Kr and Xe are found [although at higher temperatures

Table 2. Isotopic composition of new xenon component in Murchison meteorite sample 1C10. Calculated values for s-process nucleosynthesis are given in the last four lines.

Temperature (°C)	128	129	130*	131	132
1200	0.37 ±.20	-0.5 ±1.7	≡1	1.2 ±1.3	2.6 ±1.6
1400	0.43 ±.07	0.08 ±.40	≡1	0.53 ±.31	1.92 ±.37
1600	0.47 ±.12	-0.2 ±0.9	≡1	0.2 ±.7	2.5 ±.8
Mean†	0.43 ±.06	0.03 ±.36	≡1	0.51 ±.28	2.04 ±.33
Mean†	0.43 ±.06	0.44 ±.38	≡1	0.28 ±.22	2.02 ±.35
(42)	0.47	0.18	≡1	0.27	1.5
(13, 43)	0.33	0.14	≡1	0.39	2.50
(13, 44)	0.60	0.22	≡1	0.24	1.50
(13, 45)	0.79	0.33	≡1	0.39	1.60

*Concentrations of the new component in the various temperature fractions, in units of $10^{-10} \text{ cm}^3 \text{ }^{130}\text{Xe}$ per gram, are: 1100°C, 0.66; 1200°C, 0.88; 1400°C, 0.69; and 1600°C, 0.17. †The first mean is a weighted mean of the data in the table. The second mean refers to an analogous set of data, calculated for a different fission component [Murchison 2, based on a strongly mass fractionated trapped component, instead of Murchison 1, based on a lightly fractionated component (7)]. Evidently the final results are essentially similar for both choices of fission component.

Table 3. Krypton in severely etched residue 1C10 of the Murchison meteorite (9, 41). Corrections for hot blanks were negligible up to 1200°C, and were applied only to the 1400° and 1600°C fractions, where they comprised 3 and 40 percent of the observed ^{84}Kr signal (10).

Temperature (°C)	^{84}Kr ($\times 10^{-10}$ $\text{cm}^3 \text{ STP/g}$)	^{78}Kr	^{80}Kr	$^{84}\text{Kr} \equiv 100$		
				^{82}Kr	^{83}Kr	^{86}Kr
800	2730	0.607 ±.012	3.999 ±.055	20.066 ±.087	20.218 ±.065	31.12 ±.33
1000	384	0.544 ±.015	3.737 ±.071	19.23 ±.11	19.95 ±.13	32.18 ±.35
1100	166	0.545 ±.014	3.683 ±.065	19.41 ±.11	20.211 ±.081	32.33 ±.35
1200	57	0.565 ±.033	3.651 ±.080	19.40 ±.28	20.39 ±.20	31.78 ±.38
1400	9.7	0.68*	3.27 ±.10	19.89 ±.50	20.07 ±.23	31.49 ±.51
1600	1.3 ±.1	0.71*	4.39 ±.46	22.2 ±2.1	19.0 ±2.1	32.0 ±3.1
Total	3348	0.596 ±.010	3.945 ±.046	19.927 ±.072	20.189 ±.055	31.31 ±.27

*Average of first two peak height measurements only.

than Ne-E in other meteorites [16]). In stellar nucleosynthesis, neon is made by helium burning rather than by the s process, but both processes are believed to take place in red giants (17).

Argon shows a slight rise in the $^{36}\text{Ar}/^{38}\text{Ar}$ ratio with increasing temperature (Table 4), but the ratios for the 1400° and 1600°C fractions agree with the solar and terrestrial value of 5.32 within the limits of error. Helium, on the other hand, shows a significant trend. The $^4\text{He}/^3\text{He}$ ratios for the 800° to 1100°C fractions rise from 6900 to 10,100, well above the solar value of 2500. The drift toward higher values may represent release of small amounts of cosmogenic $^3\text{He}_c$, judging from the concurrent release of cosmogenic $^{21}\text{Ne}_c$ (Fig. 3). A correction for $^3\text{He}_c$ can be estimated from the $^{21}\text{Ne}_c$ content, but since He diffuses faster than Ne, this correction can only be applied to all three fractions combined. Proceeding in the conventional manner (7) we find $^{21}\text{Ne}_c = 1.8 \times 10^{-9} \text{ cm}^3 \text{ STP/g}$, which, assuming $(^3\text{He}/^{21}\text{Ne})_c = 5$, yields $^3\text{He}_c = 9 \times 10^{-8} \text{ cm}^3 \text{ STP/g}$, or 7 percent of the observed ^3He . The corrected $^4\text{He}/^3\text{He}$ ratio in the 800° to 1100°C interval thus is 8400, close to the ratio of 7000 ± 1000 for "planetary" helium (18).

The $^4\text{He}/^3\text{He}$ ratios for the 1200° and 1400°C fractions decline sharply, to 2300 and 500 (Table 4). The neon data tell us that this drop is not due to cosmogenic $^3\text{He}_c$, because there is little ^{21}Ne and even less $^{21}\text{Ne}_c$ in these fractions, and $^3\text{He}_c$ should have escaped before $^{21}\text{Ne}_c$ anyway. [This argument would not hold if diamond were the host phase, because meteoritic diamond has a high $(^3\text{He}/^{21}\text{Ne})_c$ production ratio and a high release temperature (19). However, there is no

diamond in Murchison.] Apparently the low $^4\text{He}/^3\text{He}$ ratio is an integral part of the isotopic anomalies in the high-temperature fractions of 1C10.

There are few astrophysical processes that will produce ^3He without unobserved side effects such as ^{21}Ne ; interestingly, one of them is hydrogen shell burning in red giants (17, 20). For stars of 1 to 1.5 solar masses, $^4\text{He}/^3\text{He}$ ratios as low as 200 are attained (20). Thus all four isotopic anomalies found in Murchison 1C10 can be assigned, with varying de-

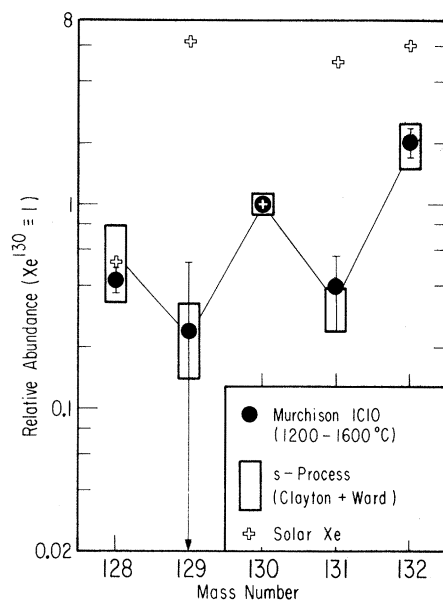


Fig. 2. New xenon component (circles) shows three attributes of xenon synthesized by the s process [rectangles; from (13)]: predominance of even over odd isotopes, increase in abundance with mass number, and rarity or absence of the very light and heavy isotopes, 124 to 126 and 134 to 136. Solar xenon (crosses) shows quite a different trend, with the odd isotopes 129 and 131 being more abundant than their even neighbors, 128 and 130.

Table 4. Helium, neon, and argon in severely etched residue IC10 of the Murchison meteorite (9, 41). The data have been corrected for spectrometer background and hot blanks. The latter were determined at 1200°, 1400°, and 1600°C; the 1200°C value was also used at the lower temperatures. Errors shown include the uncertainties in these corrections as well as the statistical error (1 standard deviation) in the linear extrapolation of isotope ratios to zero time. For helium, peak heights of the two isotopes were used in the extrapolation instead of the isotope ratio. Errors shown for the concentrations are due to instrument background and blank only, and do not include the absolute uncertainties (He, ±20 percent; Ne and Ar, ±10 percent).

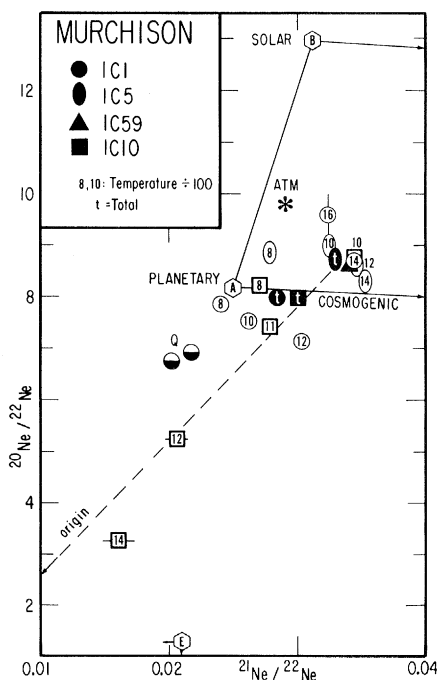
Temperature (°C)	$\frac{^4\text{He}}{^3\text{He}}$	^3He	^4He ($\times 10^{-8}$ cm ³ STP/g)	^{22}Ne	$\frac{^{20}\text{Ne}}{^{22}\text{Ne}}$	$\frac{^{21}\text{Ne}}{^{22}\text{Ne}}$	^{36}Ar ($\times 10^{-8}$ cm ³ STP/g)	$\frac{^{36}\text{Ar}}{^{38}\text{Ar}}$	$\frac{^{40}\text{Ar}}{^{36}\text{Ar}}$
800	6,900	46 ±1	318,000 ±2,000	55	8.23 ±.11	0.02701 ±.00063	3350	5.423 ±.038	0.098 ±.001
1000	8,000	76 ±1	611,000 ±2,000	135	8.78 ±.12	0.03438 ±.00085	620	5.275 ±.037	0.012 ±.002
1100	10,100	12 ±1	121,000 ±2,000	103	7.42 ±.10	0.02977 ±.00061	310	5.234 ±.037	0
1200	2,250	16 ±1	36,000 ±2,000	30	5.244 ±.079	0.02056 ±.00096	100	5.344 ±.038	0.001 ±.010
1400	500	7 ±1	3,200 ±2,000	9.5	3.270 ±.078	0.0160 ±.0010	14	5.385 ±.064	0
1600		0		0.4 ±0.1	3.6 ±1.6	0.058 ±.023	1.2 ±.1	5.49 ±.72	45 ±12
Total	6,940 ±310	157 ±3	1,089,000 ±5,000	333	7.78 ±.10	0.02998 ±.00061	4395	5.386 ±.038	0.089 ±.003

degrees of certainty, to red giants: Kr and Xe to the *s* process, Ne to helium burning, and He to hydrogen shell burning.

We cannot say much about the mineralogical location of the anomalous component. X-ray diffraction of IC10 showed mainly chromite and minor spinel, with indications of some amorphous material: presumably residual organic polymer or amorphous carbon. Chromite and polymer can be ruled out as carriers on the basis of other Murchison samples, where these phases had been enriched or depleted (6, 7). The polymer outgasses at ≤ 800°C (7), whereas chromite loses its highly distinctive xenon component mainly at 1200° to 1400°C (7). Spinel and amorphous carbon have not been studied in Murchison, but at least in the C3V chondrite Allende they have the wrong properties. Allende spinel contains only negligible amounts of noble gases (6), whereas Allende carbon contains a CCFXe component (4, 6) and releases its gases at ~1000°C when chromite is present, apparently because of a chemical reaction with chromite (21). However, we do not consider it safe to generalize from one meteorite class to another, and therefore regard spinel and amorphous carbon as definite candidates. A third candidate is hibonite, CaAl₁₂O₁₉. Although not detected in our sample, it occurs in Murchison in trace amounts (22), and would probably survive our chemical treatment. Further work is obviously needed to resolve this matter. In any event, since chromite accounts for about 80 percent of the similar sample IC59 (7), which represented 0.17 percent of the meteorite, the host phase of the new component probably comprises no more

than 3×10^{-4} of the mass of the meteorite.

One or the other of these minerals is likely to be among the first phases to condense from the expanding envelope of a red giant. Pressures in the condensation region are estimated to be 1 to 10^3 dyne/cm² (23), so that condensation



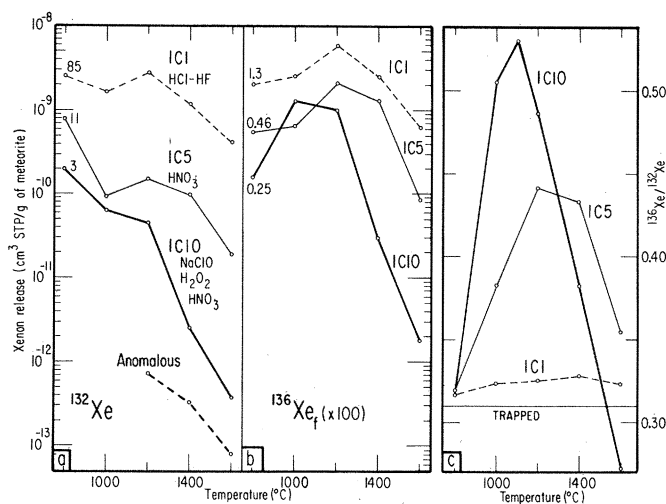
of Xe, Kr, Ne, and He are related to some of the other isotopic anomalies recently discovered in carbonaceous chondrites, involving O (27), Mg (28), Si (29), Ca (30), S (31), Ba (32), Nd (32, 33), and Sm (33). All of the earlier anomalies have been found in high-temperature minerals, and although the host phase of the new anomaly has not yet been identified, a high-temperature mineral seems again to be implicated by the high release temperatures and by the elimination of other known constituents of the sample. Such refractory phases are expected to be the first stellar condensates (24, 26), and have the best chance of surviving formation of the solar system without melting or vaporization. Thus one might expect them to retain evidence of presolar nuclear processes (27, 34).

By the same token, the CCFXe anomalies are not likely to be presolar. CCFXe is more abundant (10^{-2} rather than 5×10^{-5} of the total Xe in the meteorite); it occurs in the matrix, not the high-temperature inclusions; its host phases chromite, carbon, and Q are secondary, low-temperature minerals; and these phases or their associated trace elements such as Pb or Os have typical solar-system, not exotic, isotopic compositions (6, 35). Thus carbon, one of the main carriers of CCFXe, has a $^{12}\text{C}/^{13}\text{C}$ ratio of 90.4 (6), well within the terrestrial range of 88 to 94 but much above the typical ratio of ~ 40 for interstellar clouds (36). The origin of CCFXe must probably be sought in local processes in the early solar system (4-6).

A potentially interesting clue is the low $^{82}\text{Kr}/^{130}\text{Xe}$ ratio of the new component: 0.2 to 0.3, two orders of magnitude below the solar-system value of 24. Much or all of the difference may reflect a chemical effect, namely preferential trapping of Xe. This effect has been seen in terrestrial shales [6- to 800-fold decrease in Kr/Xe below the atmospheric value (37)] and in meteoritic minerals [~ 10 - to 25-fold decrease below the solar ratio (7)]. It is conceivable, however, that part of the difference has a nuclear cause: an *s* process involving neutron fluences higher than that which made the bulk of the solar-system nuclides [4.8 neutrons per iron seed nucleus (38)]. Such a process would enhance the Ba-Xe peak relative to the Sr-Kr peak.

Some late-type stars indeed show such enhancements. Three CH stars that are strongly enriched in heavy elements have Ba/Y ratios 6 to 13 times greater than solar (14, 39), apparently because of the operation of an *s* process with 70 neutrons per Fe nucleus (39). Whether

Fig. 4. Xenon release curves of mineral residues from the Murchison meteorite. Numbers at left of the curves give the total xenon content of each sample, in units of 10^{-10} cm³ STP/g of meteorite. (a) Etching of the original HCl-HF residue (1C1) with HNO₃ removes most of the trapped xenon, and leaves a sample (1C5) consisting mainly of chromite and residual polymer. Treatment with alkaline oxidants (1C10) to remove the polymer has only a moderate effect on the 800° to 1200°C fractions, but greatly lowers the release in the 1400° to 1600°C interval, enabling a new, anomalous Xe component to show. (b) Release of $^{136}\text{Xe}_t$, representing the CCF component residing mainly in chromite, shows that the emergence of the anomalous component in 1C10 was aided by a shift of the peak to lower temperatures. (c) Preferential removal of the trapped component is illustrated by progressive increase in $^{136}\text{Xe}/^{132}\text{Xe}$ on etching. A shift of the 1C10 peak to lower temperatures is also evident.



such an unusual *s* process needs to be invoked for Murchison may be learned from measurements of other, less volatile elements in the Ba and Sr peaks. It would be surprising if this turned out to be the case, because it would mean that ejecta from a single red giant in the solar neighborhood dominated over the average interstellar background. Moreover, high $^3\text{He}/^4\text{He}$ ratios are produced only in stars of low mass, which evolve very slowly (20) and thus would not, except by a rare coincidence, have reached the red giant stage just when the solar system was about to form.

The new anomalies constitute the first evidence for unhomogenized *s*-process matter in primitive solar-system matter, previous anomalies having been attributed to the *r* process or to explosive nucleosynthesis in a supernova. Indeed, since the new anomalies are large and unambiguous, it may be profitable to reconsider earlier interpretations, now that evidence for an additional process has been found.

After four decades dominated by the dogma of an isotopically and chemically uniform early solar system, isotopic anomalies are now being discovered in primitive meteorites at an accelerating pace. It is remarkable that products of one or more stellar nucleosynthesis events have survived in meteorites, and although the signals are often small, sporadic, and entangled with each other, the number of anomalies already exceeds the number of possible processes. Thus there is hope that unique and specific answers to the nuclear prehistory of the solar system will ultimately emerge. Mean-

while, credit must be given to workers who anticipated the survival of presolar matter in meteorites (3, 16, 34, 40), although not all their expectations have been borne out.

B. SRINIVASAN*, EDWARD ANDERS
Enrico Fermi Institute and Department
of Chemistry, University of Chicago,
Chicago, Illinois 60637

References and Notes

1. J. H. Reynolds and G. Turner, *J. Geophys. Res.* **69**, 3263 (1964).
2. U. Frick and R. K. Moniot, *Geochim. Cosmochim. Acta Suppl.* **8** (1977), p. 229.
3. O. K. Manuel, E. W. Hennecke, D. D. Sabu, *Nature (London) Phys. Sci.* **240**, 99 (1972); D. D. Sabu and O. K. Manuel, *Nature (London)* **262**, 28 (1976).
4. R. S. Lewis, B. Srinivasan, E. Anders, *Science* **190**, 1251 (1975).
5. E. Anders, H. Higuchi, J. Gros, H. Takahashi, J. W. Morgan, *ibid.*, p. 1262.
6. R. S. Lewis, J. Gros, E. Anders, *J. Geophys. Res.* **82**, 779 (1977).
7. B. Srinivasan, J. Gros, E. Anders, *ibid.*, p. 762.
8. J. Gros and E. Anders, *Earth Planet. Sci. Lett.* **33**, 401 (1977); M. Christophe Michel-Levy, B. Cervelle, C. Desnoyers, *Bull. Soc. Fr. Mineral. Cristallogr.* **100**, 258 (1977).
9. A sample of the Murchison meteorite was treated alternately with 1M HCl-10M HF and 3M HCl until a residue of 2.23 percent remained, designated 1C1 (7). A 46.5-mg portion of 1C1 was alternately treated with 3M NaOH-0.3M NaClO (80°C, 5 hours) and 6M NaOH, with gradual addition of 30 percent H₂O₂ (25°C, 2 hours; 80°C, 1 hour), to oxidize the organic polymer. After two such cycles, the sample was washed with water and dilute HCl, and etched with 21M HNO₃ (55°C, overnight), to remove the principal gas-bearing phase, Q. Another NaOH-NaClO, NaOH-H₂O₂ cycle, followed by an HNO₃ etch, yielded a residue of 4.87 mg, designated 1C10.
10. The isotopic composition of the blank was ill-determined and was assumed to be atmospheric. The uncorrected values for the 1600°C fraction, following the mass numbers of the isotopes, are: 78, 0.67 ± 0.20; 80, 4.22 ± 0.14; 82, 21.40 ± 0.36; 83, 19.44 ± 0.61; 86, 31.44 ± 0.50; 124, 0.512; 126, 0.423; 128, 10.08 ± 0.59; 129, 82.5 ± 4.4; 130, 20.7 ± 1.1; 131, 66.3 ± 3.7; 134, 32.38 ± 0.74; and 136, 28.51 ± 0.71.
11. Although CCFXe consists of two components of manifestly different origins, they show only slight, occasional separation in the laboratory

- (6, 12), and hence tend to act as one component. Similarly, the two minerals in each pair contain components that are either indistinguishable [CCFXe in chromite and carbon (6)] or very similar [trapped xenon in polymer and Q (7)], and so even samples of quite diverse mineralogy still tend to lie on the mixing line.
12. R. S. Lewis, L. Alaerts, E. Anders, in *Lunar Science IX* (Lunar Science Institute, Houston, 1978), p. 645.
 13. D. D. Clayton and R. A. Ward, *Astrophys. J.*, in press.
 14. A. G. W. Cameron, *Space Sci. Rev.* **15**, 121 (1973).
 15. Krypton-86 is a mixture of trapped and fission components only, of the isotopic composition given in (7). The amount of the fission Kr component is calculated from the fission Xe component found previously, using an $^{86}\text{Kr}/^{136}\text{Kr}$ of 0.31 ± 0.09 (7).
 16. D. C. Black and R. O. Pepin, *Earth Planet. Sci. Lett.* **6**, 395 (1969); D. C. Black, *Geochim. Cosmochim. Acta* **36**, 377 (1972); P. Eberhardt, *Earth Planet. Sci. Lett.* **24**, 182 (1974); F. Niederer and P. Eberhardt, *Meteoritics* **12**, 327 (1977). The latter authors observed a $^{21}\text{Ne}/^{22}\text{Ne}$ ratio of 0.0211 in a carbonaceous fraction from the Dimmitt H3 chondrite.
 17. V. Trimble, *Rev. Mod. Phys.* **47**, 877 (1975).
 18. U. Frick, R. K. Moniot, J. M. Neil, D. L. Phinney, J. H. Reynolds, *Geochim. Cosmochim. Acta*, in press; P. M. Jeffery and E. Anders, *ibid.* **34**, 1175 (1970).
 19. R. Göbel, U. Ott, F. Begemann, *J. Geophys. Res.* **83**, 855 (1978).
 20. I. Iben, Jr., *Astrophys. J.* **147**, 624 (1967); ——— and J. W. Truran, *ibid.* **220**, 980 (1978).
 21. B. Srinivasan, R. S. Lewis, E. Anders, *Geochim. Cosmochim. Acta* **42**, 183 (1978).
 22. L. H. Fuchs, E. Olsen, K. J. Jensen, *Smithson. Contrib. Earth Sci.* **10** (1973), p. 13.
 23. R. Clegg and S. Wyckoff, *Mon. Not. R. Astron. Soc.* **179**, 417 (1977).
 24. L. Grossman and J. W. Larimer, *Rev. Geophys. Space Phys.* **12**, 71 (1974).
 25. J. W. Larimer and M. Bartholomay, *Geochim. Cosmochim. Acta*, in press.
 26. J. M. Lattimer, D. N. Schramm, L. Grossman, *Astrophys. J.* **219**, 230 (1978).
 27. R. N. Clayton, L. Grossman, T. K. Mayeda, *Science* **182**, 485 (1973); R. N. Clayton, N. Onuma, L. Grossman, T. K. Mayeda, *Earth Planet. Sci. Lett.* **34**, 209 (1977); R. N. Clayton and T. K. Mayeda, *Geophys. Res. Lett.* **4**, 295 (1977).
 28. G. J. Wasserburg, T. Lee, D. A. Papanastassiou, *Geophys. Res. Lett.* **4**, 299 (1977); T. Lee, D. A. Papanastassiou, G. J. Wasserburg, *Astrophys. J.* **211**, L107 (1977).
 29. R. N. Clayton, T. K. Mayeda, S. Epstein, in *Lunar Science IX* (Lunar Science Institute, Houston, 1978), p. 186.
 30. T. Lee, D. A. Papanastassiou, G. J. Wasserburg, *Astrophys. J.* **220**, L21 (1978).
 31. C. E. Rees and H. G. Thode, *Geochim. Cosmochim. Acta* **41**, 1679 (1977).
 32. M. T. McCulloch and G. J. Wasserburg, *Astrophys. J.* **220**, L15 (1978).
 33. G. W. Lugmair, K. Marti, N. B. Scheinin, in *Lunar Science IX* (Lunar Science Institute, Houston, 1978), p. 672; D. A. Papanastassiou, J. C. Huneke, T. M. Esat, G. J. Wasserburg, in *ibid.*, p. 859.
 34. D. D. Clayton, *Astrophys. J.* **199**, 765 (1975); *Icarus* **32**, 255 (1977).
 35. H. Takahashi, H. Higuchi, J. Gros, J. W. Morgan, E. Anders, *Proc. Natl. Acad. Sci. U.S.A.* **73**, 4253 (1976).
 36. C. H. Townes, *Observatory* **97**, 52 (1977).
 37. R. A. Canals, E. C. Alexander, Jr., O. K. Manuel, *J. Geophys. Res.* **73**, 3331 (1968); D. Phinney, *Earth Planet. Sci. Lett.* **16**, 413 (1972).
 38. R. A. Ward, M. J. Newman, D. D. Clayton, *Astrophys. J. Suppl. Ser.* **31**, 33 (1976); D. D. Clayton, W. A. Fowler, T. E. Hull, B. A. Zimmerman, *Ann. Phys. (N.Y.)* **12**, 331 (1961).
 39. P. Lee, *Astrophys. J.* **192**, 133 (1974).
 40. R. N. Clayton, *Science* **140**, 192 (1963); A. G. W. Cameron, in *Interstellar Dust and Related Topics*, J. M. Greenberg and H. C. Van de Hulst, Eds. (Reidel, Dordrecht, 1973), p. 545; ——— and J. W. Truran, *Icarus* **30**, 447 (1977).
 41. A 4.72-mg sample of Murchison residue 1C10 was heated for 30 minutes at each of the temperatures indicated, to extract noble gases. Concentrations are accurate to ± 20 percent for He and ± 10 percent for all other gases.
 42. P. A. Seeger, W. A. Fowler, D. D. Clayton, *Astrophys. J. Suppl. Ser.* **11**, 121 (1965).
 43. B. J. Allen, J. H. Gibbons, R. L. Macklin, *Adv. Nucl. Phys.* **4**, 205 (1971).
 44. J. A. Holmes, S. E. Woosley, W. A. Fowler, B. A. Zimmerman, *At. Data Nucl. Data Tables* **18**, 305 (1976).
 45. V. Benzi, R. d'Orazi, G. Reffo, M. Vaccari, unpublished work cited in (13).
 46. We are indebted to J. Gros for preparation of the sample, to R. S. Lewis for the x-ray diffraction pattern, and to D. N. Schramm for advising us of some potential paradoxes raised by our data. One of us (B.S.) thanks the University of Missouri for releasing time to allow completion of this report. This work was supported in part by NASA grant NGL-14-001-010.

* Present address: Department of Chemistry, University of Missouri, Rolla 65401.

8 February 1978

Seismic Amplitude Measurements Suggest Foreshocks Have Different Focal Mechanisms than Aftershocks

Abstract. *The ratio of the amplitudes of P and S waves from the foreshocks and aftershocks to three recent California earthquakes show a characteristic change at the time of the main events. As this ratio is extremely sensitive to small changes in the orientation of the fault plane, a small systematic change in stress or fault configuration in the source region may be inferred. These results suggest an approach to the recognition of foreshocks based on simple measurements of the amplitudes of seismic waves.*

Significant progress has been made in the recognition of long-term recurrence patterns of large earthquakes (1), and promising results are slowly accumulating which suggest that intermediate-term changes (years to months) in regional seismicity, strain, and electromagnetic measurements may provide intermediate-term precursors (2, 3). However, the fact remains that short-term precursors (days to hours) will be needed to allow evacuation of unsafe structures, if significant reductions are to be made in loss of

life and human suffering. The recent Chinese success in predicting the Haicheng earthquake (4 February 1975, magnitude $M = 7.3$) was based on the use of long-, intermediate-, and short-term precursors. The imminent prediction was based partly on the recognition of a swarm of small to moderate earthquakes near Haicheng as a potential foreshock sequence (4). However, foreshocks do not always occur; estimates on their frequency vary widely (3, 5, 6), and they are usually recognizable as foreshocks

only in hindsight. To use foreshocks in a predictive mode, one must distinguish them from background seismicity and earthquake swarms (7).

In earlier work along the line reported here, Nersesov and his colleagues found large changes in the orientation of focal mechanisms over a large region prior to thrust earthquakes in Central Asia (8). Similar changes have recently been reported prior to an earthquake of magnitude 5 in the Central Aleutians (9). A retrospective study of the Haicheng foreshocks indicates that they were distinguishable from similar earthquake swarms on the basis of remarkably consistent focal plane solutions (4, 10). Other possible changes in compressional or shear wave amplitudes, or both, before large earthquakes have been reported from Kamchatka and China (11).

We summarize here work on small foreshocks to three moderate California earthquakes (Fig. 1, a to d) which shows that the mean nodal plane orientations were different from those of comparable aftershocks (12). In each case the inferred changes were small (5° to 10°) and were inferred from changes in the ratio of compressional to vertically polarized shear-wave amplitudes (P/SV), as recorded from nearby short-period vertical seismometers. Unfortunately, it was not possible to find small earthquakes prior to the foreshocks at the same location with which to establish "normal" background values. Therefore, it is not possible to assess whether our observations would have been of use in identifying the foreshocks as such in advance, but only that they can be used to distinguish foreshocks from aftershocks. Our observations do demonstrate, however, a simple procedure for monitoring small changes in the fault plane orientations of local earthquakes. This procedure may provide an approach to the observation of stress changes at depth preceding, accompanying, and following large earthquakes, a problem that lies directly at the core of the earthquake prediction question.

The Oroville earthquake (local magnitude $M_L = 5.7$) occurred at 2020 Greenwich mean time (G.M.T.) on 1 August 1975, in the western foothills of the Sierra Nevada, 15 km south of the town of Oroville, California. The aftershocks occurred within a planar band striking north-south and dipping steeply to the west; fault plane solutions indicate predominantly normal dip-slip motion on this plane (13). The main shock was preceded by 58 recorded foreshocks over a period of 4 weeks, starting on 28 June. They ranged from $M_L = 0.5$ to $M_L = 4.7$